Junya Konno[1] / Atsushi Nezu[2,3] / Haruaki Matsuura[4] / Hiroshi Akatsuka[1,3]

Excitation Kinetics of Oxygen O(^{1}D) State in Low-Pressure Oxygen Plasma and the Effect of Electron Energy Distribution Function

[1] Department of Energy Sciences, Tokyo Institute of Technology, Meguro, Tokyo 152-8550, Japan, E-mail: hakatsuk@lane.iir.titech.ac.jp
[2] Technical Department, Tokyo Institute of Technology, Meguro, Tokyo 152-8550, Japan
[3] Laboratory for Advanced Nuclear Energy, Institute of Innovative Research, Tokyo Institute of Technology, Meguro, Tokyo 152-8550, Japan, E-mail: hakatsuk@lane.iir.titech.ac.jp
[4] Department of Nuclear Safety Engineering, Tokyo City University, Setagaya, Tokyo 158-8557, Japan

Abstract:
We develop numerical model to discuss the number density and excitation kinetics of O(^{1}D) state in low-pressure discharge oxygen plasma. The governing equations are the Boltzmann equation to describe the electron energy distribution function and the rate equations of the relevant excited states. We have calculated them back and forth until self-consistent solution is obtained. When the rate coefficient of the electron impact dissociation of O_2 to O(^{3}P) and O(^{1}D) atoms is assumed to be functions of electron temperature T_e with Maxwellian electron energy distribution, the obtained results are found to be inappropriate. When the rate coefficients are written as functions of electron energy distribution function, satisfactory results are obtained as number density distribution of excited states. We also experimentally examined and confirmed the validity of the model by actinometry measurement for number density of the O(^{3}P) state. It is found that we should consider the electron energy distribution function in describing the excitation kinetics of O(^{1}D) state in low-pressure oxygen plasma.

Keywords: oxygen plasma, number density of excited states, metastables, electron energy distribution function, actinometry measurement, oxygen singlet D state

DOI: 10.1515/jaots-2017-0002

Received: January 3, 2017; **Revised:** January 3, 2017; **Accepted:** January 4, 2017

1. Introduction

Low-pressure oxygen plasma is now widely applied as an atomic oxygen source in advanced oxidation process of semiconductor engineering, such as ashing of photoresist, chamber cleaning, fabrication of gate oxide thin film, etc. [1, 2]. In these advanced oxidation processes, several papers reported that the O(^{1}D) atom, a metastable state of oxygen atom as the first excited state, should play a more essential role than O(^{3}P), the ground state oxygen atom, to improve the electronic quality of the gate oxide films [3, 4]. Although we also studied the excitation chemical kinetics of nitrogen/oxygen atoms and molecules in the low-pressure discharge nitrogen-oxygen mixture plasma [5, 6], we did not include the O(^{1}D) state in our previous model [4], which should be definitely taken into account to the kinetic modeling for better understanding of the plasma oxidation processes for semiconductors. This is the main objective of the present study.

In addition to the inclusion of O(^{1}D) state to the kinetic model, we would like to consider the effect of the electron energy distribution function (EEDF) in the excitation kinetics of the oxygen plasma. Namely, excitation kinetics in plasma has been often discussed in terms of electron temperature of the plasma. However, in the excitation kinetics of the plasma in a state of non-equilibrium, we must always notice the essentiality of the EEDF [7, 8], and consequently, we would like to discuss the effect of the EEDF on the number densities of the excited states as well as on the excitation kinetics itself. In other words, in the non-equilibrium plasmas, we should describe the rate equations in terms of the rate coefficients calculated with the EEDF and the corresponding cross sections, and the rate coefficients should not be considered as functions of the electron temperature [1, 2, 5–8]. We would like to confirm this kind of essentiality of the EEDF in the non-equilibrium oxygen plasma, which

Hiroshi Akatsuka is the corresponding author.

is the second objective of this study. For this purpose, we will carry out experiments to crosscheck the numerical modeling to describe the number density of some of the oxygen species. Namely, we will carry out optical emission spectroscopic (OES) measurement of number density of the oxygen atom situated at the ground state, i. e., O(^{3}P) state, by actinometry measurement in order to confirm the role of the EEDF in the excitation kinetics [4, 5].

2. Numerical modeling of chemical kinetics of excited species in oxygen plasma

In the present study, as a principal objective, we discuss the chemical kinetics of several essential excited species in a steady-state discharge oxygen plasma with its discharge pressure 1 – 5 Torr. We choose this discharge pressure region because the field effect transistor (FET) gate oxidation process is carried out with the oxygen discharge plasma under this pressure condition [1, 2]. And in the present study, we include following nine species in our numerical modeling to obtain their number densities in the steady-state oxygen discharge, i. e., O_2(X $^3\Sigma_g^-$), O_2(a $^1\Delta_g$), O_2(b $^1\Sigma_g^+$), O^-, O_3, O_2^+, O(^{3}P), O(^{1}D), and e^- (free electron). Under the present discharge condition, it is considered that we can neglect other excited species because their number densities are sufficiently low, and consequently, they do not play an important role in the population or depopulation of O(^{1}D).

The input parameters of the present kinetic modeling are the followings: (1) the total discharge pressure P to determine the total number densities in the plasma, (2) the gas temperature T_g to determine the rate coefficients of atomic or molecular chemical reactions, (3) the electron density N_e, (4) the discharge tube radius R, and (5) the reduced electric field E/N to determine the EEDF and the resultant rate coefficients or electron collision excitation or de-excitation reactions. We must notice that only four parameters are independent among the five input parameters listed above. This is physically evident because the electron density N_e, as well as number densities of each excited species, is uniquely determined when we determine the reduced electric field E/N with the discharge pressure P, the discharge tube radius, and the gas temperature T_g. Of course, the number densities of ionic species in the present modeling are also given as the functions of these input parameters, where the quasi-neutral condition must hold. That is, the number densities of the charged species calculated in the present study (O^-, O_2^+, and e^-) must keep the charge neutrality. Hence, we adjust the gas temperature T_g to keep the quasi-neutral condition just like our previous numerical study [4, 5]. From the practical point of view, when we increase the gas temperature by 10 %, we can keep this condition in our numerical modeling. Particularly, when we increase the reduced electric field, it was found that the self-consistent gas temperature also increases, which agrees with the plasma gas heating by the discharge plasma. We consider that our present numerical modeling does not contradict with the real discharge experiment in this respect.

The governing equations to describe the excitation kinetics in the oxygen plasma consists of two sets of equations: the one is a set of equations to describe the temporal evolution of number densities of excited species in the oxygen plasma, and the other is the Boltzmann equation to find the EEDF in the oxygen plasma [4–6]. Concerning the former one, the number densities of the excited species are described as the corresponding rate equations describing the population and depopulation on the basis of chemical kinetics in the plasma, which are simultaneous ordinary differential equations. These rate equations include the excitation or de-excitation reactions by the electron collisions, chemical reactions by the atomic or molecular collisions, and diffusion loss for long-life species such as the metastable states or the ground-state ions, as time-dependent ordinary differential equations, although they are not necessarily linear equations. In short, we have the following ordinary differential equations of each excited species A for its time derivative:

$$\frac{\mathrm{d}[\mathrm{A}]}{\mathrm{d}t} = -\nu_w [\mathrm{A}] + G \tag{1}$$

where [A] is the number density of the species A, ν_w is the loss frequency by collision with the discharge tube wall, G is the source term of the species A by the electron collision or by the atomic/molecular collision, where the collisional loss is considered to be a negative source term. Here, ν_w is calculated from the boundary condition, or the deactivation probability γ, on the surface of the discharge tube wall, which can be formulated as follows [4–6, 9]:

$$\nu_w = \frac{\gamma c}{2R} \quad \text{for } \gamma << 1, \tag{2}$$

$$\nu_w = \left(\frac{2.405}{R}\right)^2 D \quad \text{for } \gamma \sim 1, \tag{3}$$

where R is the inner radius of the discharge tube wall, c is the average thermal velocity and D is the diffusion coefficient of the species A. For ions, D should be considered as the ambipolar diffusion coefficient. When we

calculate the coefficient G, we assume that the heavy species, i. e., neutral particles and ions, are in the state of thermodynamic equilibrium with their gas temperature T_g, which has been confirmed by many studies and considered to be justifiable for many low-pressure gas discharge plasmas applied to practical applications [1, 2, 9]. As a radial distribution of the species, we assumed the Bessel function of the 0-th order $J_0(2.405r/R)$ for the particles with $\gamma \sim 1$ [O_2^+], whereas for the species with $\gamma << 1$ [O_2(a $^1\Delta_g$), O_2(b $^1\Sigma_g^+$), and O(^{3}P)], the uniform distribution over the discharge tube [9]. The detailed rate coefficients of the wall loss processes are the same with our previous study [4, 5]. It should be also noted that the radiative loss of excited oxygen species is negligible in the present study, which is different from the nitrogen plasma [5].

In the meantime, for the electron impact excitation or de-excitation processes, the rate coefficients k_e must be calculated by applying the following integral calculation, because the electrons generally do not obey the Boltzmann distribution [4–8]:

$$k_e = \sqrt{\frac{2}{m_e}} \int_{\varepsilon_{th}}^{\infty} \sigma(\varepsilon)\, \varepsilon f(\varepsilon)\, d\varepsilon, \tag{4}$$

where $\sigma(\varepsilon)$ is the electron collision cross section for the electron with the energy ε, m_e is the electron mass, ε_{th} is the threshold electron energy for the reaction, and $f(\varepsilon)$ is the electron energy probabilistic function (EEPF), which is given with the EEDF $F(\varepsilon)$ as follows:

$$f(\varepsilon) = \frac{1}{\sqrt{\varepsilon}} F(\varepsilon). \tag{5}$$

It indicates that we must solve the second governing equation of this modeling, that is, the Boltzmann equation to determine the EEPF of the oxygen plasma. In this equation, it should be remarked that the dissociation degree of oxygen molecule will increase as the applied reduced electric field E/N is increased. We must consider the change in the constituents of the collision counterpart of an electron, that is, the variation in the mixture ratio of O_2 molecule and O atom, because of their mass difference in the elastic collision and their reaction channel difference in the inelastic collision [4–6]:

$$-\frac{d}{d\varepsilon}\left[\frac{1}{3}\left(\frac{E}{N}\right)^2 \frac{\varepsilon}{\sum_S \delta_S \left\{\sigma_c^S(\varepsilon) + \sum_j \sigma_{sj}^S(\varepsilon)\right\}} \frac{df}{d\varepsilon} + \left\{\sum_S \delta_S \frac{2m_e}{M_S} \sigma_c^S(\varepsilon)\right\} \varepsilon^2 \left(f + \frac{kT_g}{e}\frac{df}{d\varepsilon}\right)\right] + \sum_j \varepsilon \sigma_{sj}^S(\varepsilon) f(\varepsilon) = 0, \tag{6}$$

where E/N is the reduced electric field, ${\sigma_c}^S$ is the momentum transfer collision cross section of the species S (S = 1 for O atom, S = 2 for O_2 molecule), M_S is the mass of the S-th heavy species, δ_S is the number-density fraction of the S-th heavy species, ${\sigma_{sj}}^S$ is the cross section of the j-th inelastic collision of the S-th heavy species, k is the Boltzmann constant, and e is the elementary charge. We set the unit of the electron energy as eV in Eqs. (4) – (6). We normalized the EEPF $f(\varepsilon)$ as follows:

$$\int_0^{\infty} f(\varepsilon)\sqrt{\varepsilon} d\varepsilon = \int_0^{\infty} F(\varepsilon)\, d\varepsilon = 1. \tag{7}$$

In the present study, we considered 15 electron collision reactions when we solve Eq. 1, which are summarized in Table 1. In our previous study of oxygen discharge plasma [4–6], we had considered the number density only of the O(^{3}P) state on the basis of similar numerical modeling but without O(^{1}D) state, where we took into account the electron collision reactions #1 – #11 shown in Table 1. And, in the present modeling, to calculate the number density of the O(^{1}D) state, we newly added the reactions #12 – #15 in Table 1. Some reactions with bidirectional arrows are treated not only with the forward reaction but also with the reversal one, whose cross section is calculated with the Klein-Rossland relation [5]. Unfortunately, since we could not find the cross sections of reaction #9 and #11, we used their rate coefficients given as a function of the electron temperature, where we applied the electron kinetic temperature T_{ek} to the electron temperature T_e defined as follows:

$$T_{ek} \equiv \frac{2}{3k} \int_0^{\infty} \varepsilon^{3/2} f(\varepsilon) d\varepsilon = \frac{2}{3k} \langle \varepsilon \rangle. \tag{8}$$

Table 1: List of electron collision processes considered in the calculation of number densities of excited states in eq. 1).

No.	Electron Collision Reactions			Reference
1	$O_2(X\,^3\Sigma_g^-) + e^-$	↔	$O_2(a\,^1\Delta_g) + e^-$	Capitelli et al. [9]
2	$O_2(X\,^3\Sigma_g^-) + e^-$	↔	$O_2(b\,^1\Sigma_g^+) + e^-$	Capitelli et al. [9]
3	$O_2(a\,^1\Delta_g) + e^-$	↔	$O_2(b\,^1\Sigma_g^+) + e^-$	Braginsky et al. [11]
4	$O_2(X\,^3\Sigma_g^-) + e^-$	→	$O_2^+ + 2\,e^-$	Capitelli et al. [9]
5	$O_2(X\,^3\Sigma_g^-) + e^-$	↔	$O^- + O(^3P)$	Phelps [12]
6	$O_2(a\,^1\Delta_g) + e^-$	↔	$O^- + O(^3P)$	Phelps [12], Capitelli et al. [9]
7	$O_2(X\,^3\Sigma_g^-) + e^-$	↔	$2\,O(^3P) + e^-$	Braginsky et al. [11]
8	$O_2(a\,^1\Delta_g) + e^-$	↔	$2\,O(^3P) + e^-$	Braginsky et al. [11], Capitelli et al. [9]
9	$O_2^+ + e^-$	→	$2\,O(^3P)$	Capitelli et al. [9]
10	$O_3 + e^-$	↔	$O(^3P) + O_2(X\,^3\Sigma_g^-) + e^-$	Gousset et al. [13]
11	$O^- + e^-$	→	$O(^3P) + 2\,e^-$	Lieberman et al. [1]
12	$O_2(X\,^3\Sigma_g^-) + e^-$	→	$O(^3P) + O(^1D) + e^-$	Phelps [12]
13	$O_2(a\,^1\Delta_g) + e^-$	→	$O(^3P) + O(^1D) + e^-$	Phelps [12], Capitelli et al. [9]
14	$O(^3P) + e^-$	↔	$O(^1D) + e^-$	Capitelli et al. [9]
15	$O_2(X\,^3\Sigma_g^-) + e^-$	→	$2\,O(^1D) + e^-$	Phelps [12]

The reason of this definition is based on the fact that T_{ek} defined above agrees with the electron temperature T_e when the EEPF is Maxwellian, which is given as $[2/(3k)]$ times the electron mean energy $\langle\varepsilon\rangle$.

In the meantime, we considered 15 atomic/molecular collision reactions, #16 – #30, as shown in Table 2. Among them, #16 – #27 are the reactions considered also in our previous study [4–6], whereas #28 – #30 are newly involved in the present study. Like calculations of rate coefficients of electron collision processes, the reactions with bidirectional arrows are treated not only with the forward reaction but also with the reversal one, whose rate coefficient is calculated with the equation of the detailed balance [5]. The reversal rate coefficient can be calculated with the equilibrium constant of the reaction, which is obtained from the partition function of the molecules involved [5, 10].

Table 2: List of atomic and molecular collision processes considered in the calculation of number densities of excited states in Eq. 1).

No.	Heavy Species Collision Reactions			Reference
16	$O_2(a\,^1\Delta_g) + O^-$	→	$O_3 + e^-$	Capitelli et al. [9]
17	$O_2(b\,^1\Sigma_g^+) + O^-$	→	$O(^3P) + O_2(X\,^3\Sigma_g^-) + e^-$	Capitelli et al. [9]
18	$O^- + O_2^+$	→	$O(^3P) + O_2(X\,^3\Sigma_g^-)$	Capitelli et al. [9]
19	$O_2(a\,^1\Delta_g) + O(^3P)$	↔	$O_2(X\,^3\Sigma_g^-) + O(^3P)$	Capitelli et al. [9]
20	$O_3 + O_2(X\,^3\Sigma_g^-)$	↔	$2\,O_2(X\,^3\Sigma_g^-) + O(^3P)$	Capitelli et al. [9]
21	$O(^3P) + O_3$	↔	$2\,O(^3P) + O_2(X\,^3\Sigma_g^-)$	Capitelli et al. [9]
22	$O(^3P) + O_3$	↔	$O_2(a\,^1\Delta_g) + O_2(X\,^3\Sigma_g^-)$	Capitelli et al. [9]
23	$O_2(b\,^1\Sigma_g^+) + O_3$	→	$2\,O_2(X\,^3\Sigma_g^-) + O(^3P)$	Gousset et al. [13]
24	$O_2(a\,^1\Delta_g) + O_2(X\,^3\Sigma_g^-)$	↔	$2\,O_2(X\,^3\Sigma_g^-)$	Capitelli et al. [9]
25	$O_2(a\,^1\Delta_g) + O_3$	→	$2\,O_2(X\,^3\Sigma_g^-) + O(^3P)$	Gousset et al. [13]
26	$O(^3P) + O_3$	→	$2\,O_2(X\,^3\Sigma_g^-)$	Capitelli et al. [9]
27	$O^- + O_2^+$	→	$3\,O(^3P)$	Capitelli et al. [9]
28	$O(^1D) + O(^3P)$	→	$2\,O(^3P)$	Lieberman et al. [1]
29	$O(^1D) + O_2(X\,^3\Sigma_g^-)$	→	$O(^3P) + O_2(X\,^3\Sigma_g^-)$	Lieberman et al. [1]
30	$O(^1D) + O_2(X\,^3\Sigma_g^-)$	→	$O(^3P) + O_2(a\,^1\Delta_g)$	Lieberman et al. [1]

Next, concerning the inelastic collisions in the Boltzmann equation as was shown in the second line of eq. 6), we considered the collisions described in Table 3. When we solve the Boltzmann equation for the oxygen plasma, we do not include the superelastic collisions with vibrationally excited species of O_2 molecule, which is quite different from the analysis of nitrogen plasma [5, 6, 10–12], because vibrational kinetics of O_2 molecules is not so essential for the formation of EEPF of the O_2 plasma [4].

Table 3: List of inelastic collision processes of electrons considered in the calculation of the Boltzmann equation, eq. 6).

No.	Electron Inelastic Collision Reactions			Reference
(1)	$e^- + O_2(X\ ^3\Sigma_g^-)$	→	$e^- + O_2(Y)$, Y = a $^1\Delta_g$, b $^1\Sigma_g^+$, 4.5 eV, 6.0 eV, 8.4 eV, 9.97 eV, 14.7 eV	Phelps [12]
(2)	$e^- + O(^3P)$	→	$e^- + O(Z)$, Z = ^{1}D, ^{1}S, 3s $^5S^o$, 3s $^3S^o$, 3p ^{5}P, 3p ^{3}P, 3d $^3D^o$, 3s $^3D^o$	Capitelli et al. [9]
(3)	$e^- + O_2(X\ ^3\Sigma_g^-)$	→	$e^- + e^- + O_2^+$	Capitelli et al. [9]
(4)	$e^- + O(^3P)$	→	$e^- + e^- + O^+$	Yurova et al. [14]
(5)	$e^- + O_2(X\ ^3\Sigma_g^-)$	→	$e^- + O + O^-$	Phelps [12]
(6)	$e^- + O_2(X\ ^3\Sigma_g^-; v = 0)$	→	$e^- + O_2(X\ ^3\Sigma_g^-; w = 1, 2)$	Phelps [12]

Basically, number densities of excited species other than vibrational levels are not so large, and consequently, the superelastic collisions are not essential at all for the formation of EEPF [5]. However, as we described previously, when the numerical calculation is conducted and as the system comes close to the steady state, the dissociation degree of oxygen increases indeed, which indicates that we must reconsider the variation in the collision partner of electrons in the oxygen plasma. That is, we must obtain the dissociation degree of O_2 molecule, and this must be self-consistently reflected on the Boltzmann equation. This fact indicates that we must simultaneously solve the rate equations of O_2 molecules to obtain the number density of O atoms, so that we must include the effect of the inelastic collisions with O atoms as well as with O_2 molecules to form the EEPF of the plasma. Hence, we must also include the electron inelastic collisions of O atoms as summarized in Table 3. When we solve eq. 6 numerically, we discretized the electron energy range from 0 to 40 eV by 0.1 eV, i. e., the one section of $\Delta\varepsilon$ is uniformly taken as 0.1-eV step, and the total number of energy sections is set at 400 points [4–6].

On the basis of collisions summarized in Table 1–Table 3, we simultaneously solve the rate equations eq. 1 and the Boltzmann eq. 6 until the self-consistent solutions are obtained with respect to the EEPF and the excited-state number densities, whose procedure is schematically illustrated in Figure 1. Usually, when we repeat the procedure several times, we can find the self-consistent steady-state solution. We can obtain the number densities of each excited species and the EEPF, and understand the excitation chemical kinetics in the oxygen plasma.

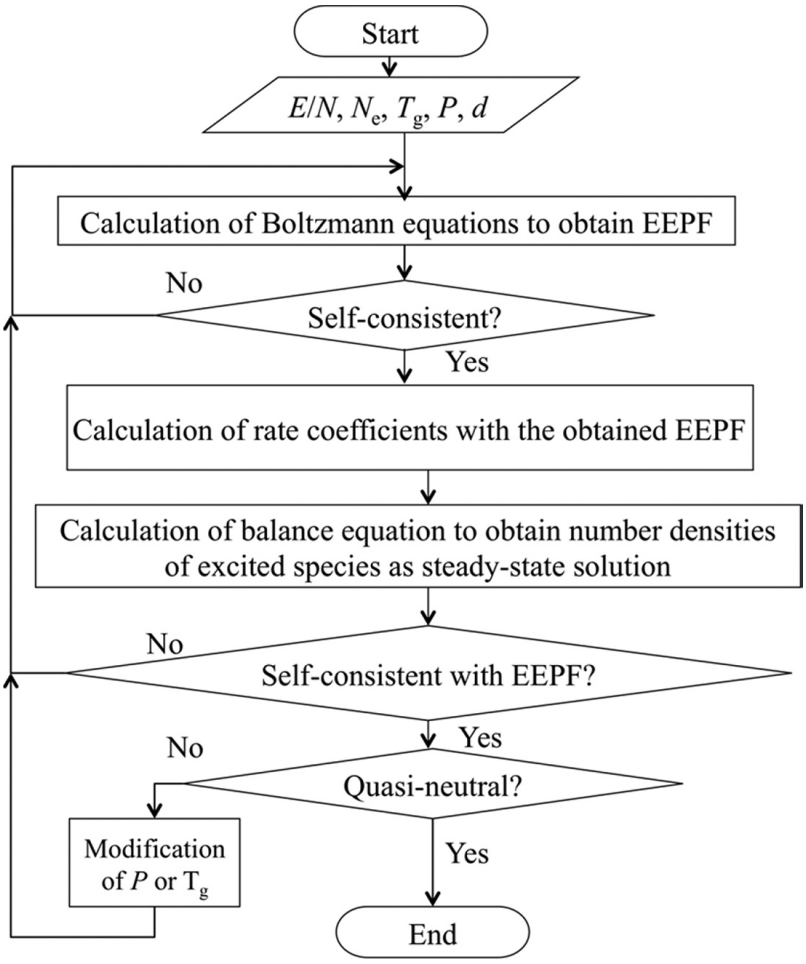

Figure 1: Schematic diagram of numerical procedure of the present calculation to determine number densities of major species in the oxygen plasma.

3. Experiments by microwave discharge oxygen plasma

Figure 2 shows a schematic diagram of the experimental setup applied in the present study, which is basically the same as was already shown in Refs. [4–8, 10, 15]. The microwave is generated by a magnetron, and transmitted to the discharge tube through the waveguide with a three-stub tuner. Its frequency is 2.45 GHz, and its output power is set at 500 W. A quartz tube of 26-mm inner diameter is inserted into the waveguide cavity with a short-circuited plunger, which acts as a discharge tube, one end of which is connected to a vacuum chamber evacuated with an oil rotary vacuum pump continuously. Oxygen gas is fed to the discharge tube with a constant flow rate and the constant evacuation, and the microwave makes the oxygen discharge plasma inside the quartz tube. The oxygen gas flow rate is set at 120 – 140 mL/min, where the discharge pressure is set at 1.0 Torr. We define the z-axis along the gas flow direction on the discharge tube with its origin at the intersection with the waveguide. We carry out actinometry measurement at z = 0, 60, 100 and 140 mm to find the ground-state atomic oxygen O(^{3}P) density with the argon atom as the actinometer, on the basis of the measurement principle described in Refs. [4, 5].

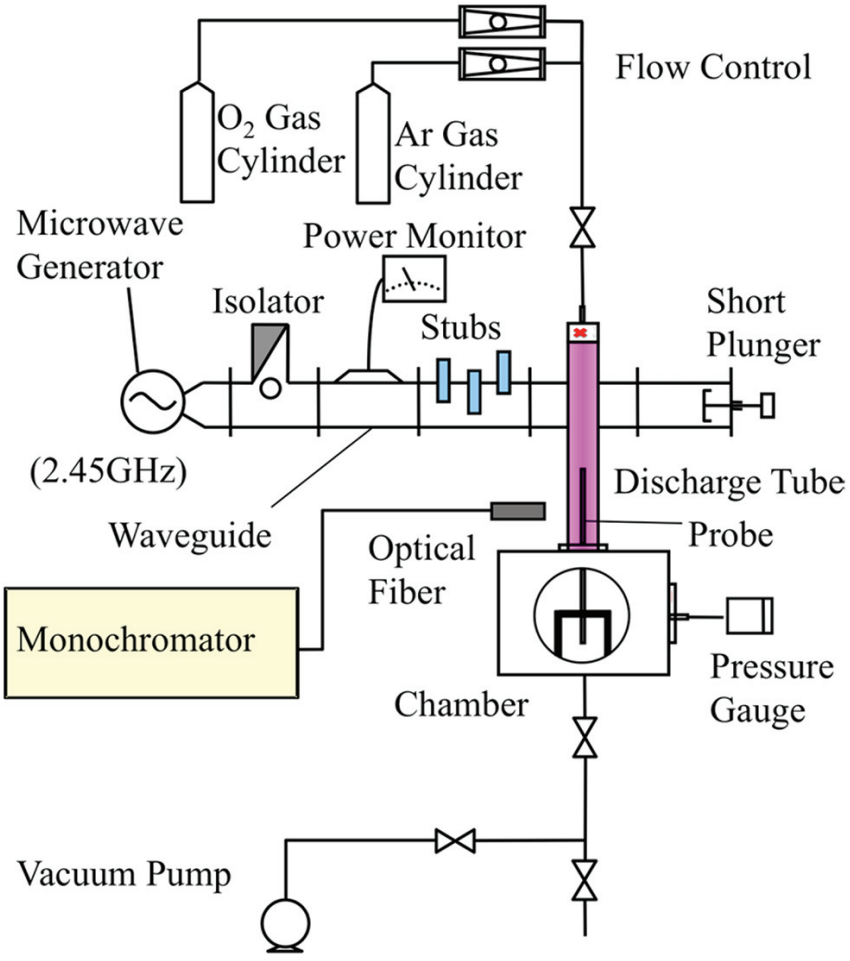

Figure 2: Schematic diagram of experimental setup of microwave discharge plasma generator.

4. Results and discussion

Figure 3 shows an example of the EEPF obtained in the present numerical simulation as explained in § 2, where we fixed the input parameters as P = 1.0 Torr, R = 1.3 cm, T_g = 1500 K, and the range of the reduced electric field E/N was set from 90 Td to 130 Td in the calculation illustrated in Figure 3. Here, the electron density was remained as an unknown parameter, which was found to be in the order of 10^{11} cm^{-3} under the given discharge

conditions. Figure 3 shows that the EEPF of the oxygen plasma in the present study becomes not a Maxwellian distribution, but a distribution with depleted high-energy component in comparison with the Maxwellian one. In other words, the high-energy tail of the EEPF shows lower temperature than the bulk energy region. The boundary electron energy, which divides the high-energy and the low-energy component, or the boundary energy at which the slope of the EEPF changes drastically, is found to be at 7 – 8 eV. This electron energy gives maximum of the cross section for the electron impact excitation of O_2 vibration, which corresponds to the reaction #(6) in Table 3. It is also found that the local temperature, which can be determined as a slope of the EEPF at the specific value of electron energy, is almost independent of the reduced electric field in the low-energy bulk region.

Next, we would like to discuss the numerical results about the number densities of the excited species in the oxygen plasma. Figure 4(a)–(b) show the number densities of each species plotted against the reduced electric field E/N under the condition of the total pressure 1 Torr with the approximate gas temperature T_g 1600 K. In Figure 4(a), since we would like to confirm the essentiality of the EEPF in the excitation kinetics in the present numerical simulation, we intentionally set the rate coefficient of the reaction #12 of Table 1 [$O_2(X\,^3\Sigma_g^-) + e^- \rightarrow O(^3P) + O(^1D) + e^-$] as follows, as the function of the electron kinetic temperature T_{ek} [1]:

$$k_e = 3.49 \times 10^{-8} \exp\left[-\frac{5.92}{(kT_{ek})\,[\mathrm{eV}]}\right]. \quad (\mathrm{cm}^3 \bullet \mathrm{sec}^{-1}) \tag{9}$$

On the other hand, in Figure 4(b), the rate coefficient of the reaction #12 of Table 1 is calculated with the electron impact excitation cross section [13] by integral calculation eq. 4 where the EEPF is simultaneously calculated with eq. 6 as a self-consistent one. When we examine Figure 4(a), it is found that the number density ratio of the atomic oxygen $O(^1D)/O(^3P)$ 0.013 – 0.014, which seems a little too low in comparison with Kitajima et al.'s report [3] or other similar works. On the other hand, when we calculate the rate coefficient with the self-consistent EEPF as was shown in eq. 6), the number density ratio $O(^1D)/O(^3P)$ is found to be about 0.032 – 0.035 (See Figure 4(b)), which is consistent with the experimental studies under similar discharge conditions. This finding indicates the essentiality of the EEPF in the discussion of excitation kinetics in the plasma.

In addition, in Figure 4(b), we can find that the density of oxygen negative ion O^- becomes larger than the electron density as lowering the reduced electric field as $E/N = 90$ Td, which also agrees with the general experimental results of low-pressure oxygen plasma [1, 3]. However, in Figure 4(a) where the rate coefficient of reaction #12 is treated as the electron kinetic temperature T_{ek}, we cannot find such tendency. The result shown in Figure 4(b) is obtained because the high-energy component of the EEPF becomes rapidly depleted as the electron energy becomes higher for the low-reduced electric field discharge. In other words, if we treat the EEPF as a Maxwellian one, then the rate coefficient of the reaction #12 becomes unrealistically large, and consequently, the number density of $O(^3P)$ becomes also unrealistically high, which results in the unrealistic high rate of the reversal reaction of the reactions #5 – #6, which decompose the oxygen negative ion O^-. This is really an undesirable numerical result, which indicates one aspect of the crucial roles of the EEPF to determine the excitation kinetics. In short, we must consider the effect of the non-Maxwellian EEPF in the present discussion in the excitation kinetics of the oxygen plasma.

In the present study, we carried out the numerical simulation of the excitation kinetics of oxygen plasma including the population and depopulation of $O(^1D)$ state. This state is, indeed, essential for the excitation kinetics, particularly for the theoretical description of the dissociation degree of the oxygen molecule, which we confirmed as follows. Figure 5 shows the dependence of the collision cross sections of the reactions #7 (to form two ground state $O(^3P)$ atoms) and #12 (to form one $O(^3P)$ and one $O(^1D)$), the electron impact dissociation processes of O_2 molecule, on the electron energy [12, 13]. Obviously, although the threshold electron energy of the reaction #12 is higher than that of the reaction #7, the absolute value of the cross section #12 is much higher than that of the reaction #7 around $\varepsilon \geq 8$ eV. This fact indicates that the atomic oxygen is more frequently produced as a pair of $O(^3P)$ and $O(^1D)$ atoms than two ground-state oxygen atoms $O(^3P)$. Therefore, it is concluded that the present kinetic modeling can improve our previous kinetic model of the oxygen plasma where only the ground state $O(^3P)$ was included as an oxygen atom [4].

Next, our interest is addressed to the electron density N_e and the dissociation degree of oxygen molecule, since they are easily compared with the experimental results and convenient for the confirmation of the validity of the excitation-kinetic model of the plasma. In addition, since the electron temperature is always the common interest among the plasma research society as one of the fundamental parameters, we would also like to pay attention to the obtained electron kinetic temperature T_{ek}. Figure 6 shows the numerically calculated relationship between the electron density N_e and the dissociation degree of O_2 molecule, which also shows the monotonic increase of dissociation with increasing electron density. Here, N_e is measured with a Langmuir double probe on the axis of the discharge tube, and the dissociation degree with actinometry measurement. We chose the electron density for the horizontal axis of Figure 6 rather than the electron kinetic temperature, since it cannot be measured directly for the plasma with non-Maxwellian EEPF. Unfortunately, the quantitative

agreement between them is not good in Figure 6, and the discrepancy about factor 3 is found. However, the monotonic increase of the dissociation degree was traced with increasing electron density, and its relative increment with N_e is reproduced in the present model fairly well. One of the reasons for this disagreement is the assumption of the radial dependence of the electron density in the present numerical modeling, i. e., the Bessel J_0 distribution of the electron density, whereas several experiments showed that the real electron distribution was rather flat over the discharge tube, or that the electron density of the inner side is rather lower in the microwave discharge tube [16]. Another possible reason lies in the experimental side, that is, the interpretation of the actinometry measurement where we inevitably assume the corona equilibrium for the actinometry level of the oxygen atom, even though we include the quenching process of the actinometric level by collisions with the background molecules because of rather high-discharge pressure, 1 Torr [4, 5]. However, it is widely noticed that the absolute determination of the number density of atoms is still difficult by the actinometry measurement in the molecular gas discharge plasmas. In the present study, it is found that the order of the dissociation degree agrees with the experiments, and that the tendency of increase with the electron density also agrees with them. Consequently, it is considered that the present numerical modeling is qualitatively reasonable [4, 5].

As a final discussion, we should specify the desirable condition for the effective generation of the $O(^1D)$ state, which is the essential species for the oxidation process for the gate oxide film preparation. Figure 4(b) shows that the dissociation degree of O_2 molecule is surely enhanced with the reduced electric field E/N. However, the ratio of $O(^1D)$ atom density to $O(^3P)$ is not much improved with the reduced electric field. Meanwhile, Figure 7 shows the pressure dependence of main excited species in the oxygen plasma under the constant reduced electric field $E/N = 110$ Td. From this figure, it is found that the relative density of the molecular singlet states like $O_2(a\ ^1\Delta_g)$ or $O_2(b\ ^1\Sigma_g^+)$ states with respect to the ground state $O_2(X\ ^3\Sigma_g^-)$ does not depend on the discharge pressure so much. The total dissociation degree is not so strongly dependent on the discharge pressure, either. Moreover, the next finding is one of the most remarkable. That is, if we would like to increase the relative density of the $O(^1D)$ state in the oxygen plasma with respect to the ground state oxygen atom with its discharge pressure about several Torr, the discharge pressure should be as low as possible.

The reason for this pressure dependence of $O(^1D)/O(^3P)$ number density ratio mainly lies in the quenching of $O(^1D)$ metastable state to the ground state $O(^3P)$ by collisions with $O_2(X\ ^3\Sigma_g^-)$ states as well as with $O(^3P)$ atoms owing to the high pressure, as was already shown in reactions #28 – #30 of Table 2. To summarize, we must operate our oxygen plasma source by reflecting the desirable conditions for each plasma treatment in the process. Although our present modeling remains a rather simple global model to describe the excitation kinetics of excited oxygen species and its level may remain as a qualitative one, it is still useful to examine the optimum operation condition of oxygen plasma source for various plasma oxidation processes for microelectronics.

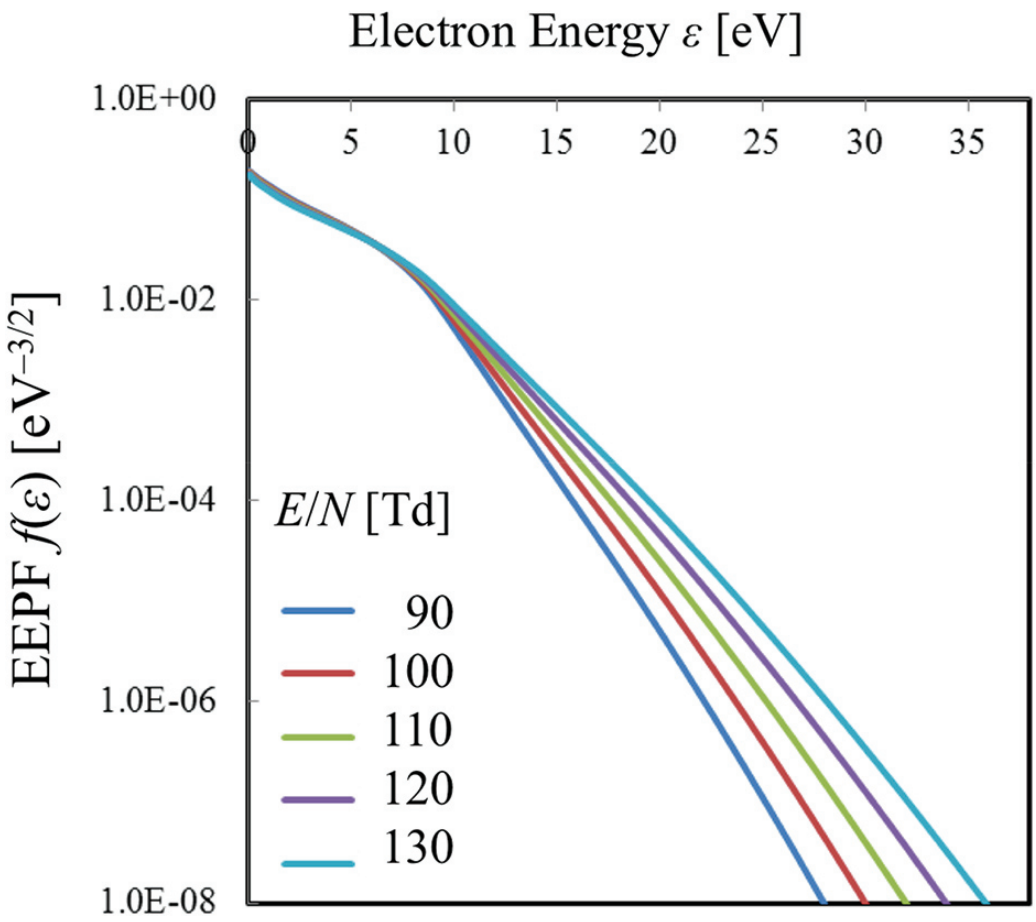

Figure 3: Numerical result of self-consistent EEPF plotted against the given reduced electric field E/N.

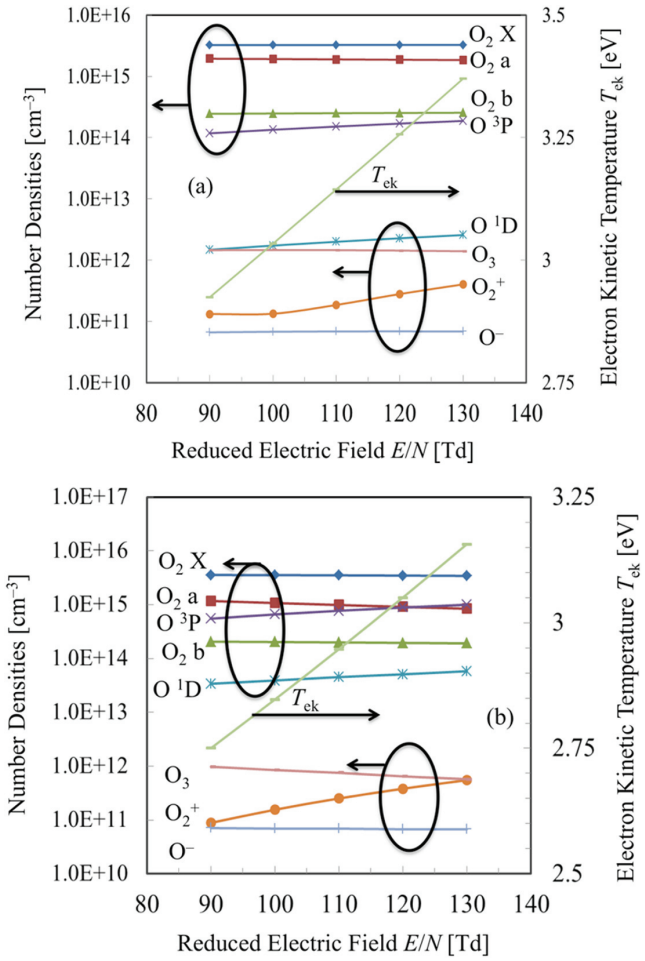

Figure 4: Number densities of various species in oxygen plasma calculated as functions of reduced electric field, where the rate coefficient of reaction No. 12 in Table 1 is treated as a function of T_e in (a), whereas calculated by eq. 4 with the cross section and EEPF in (b).

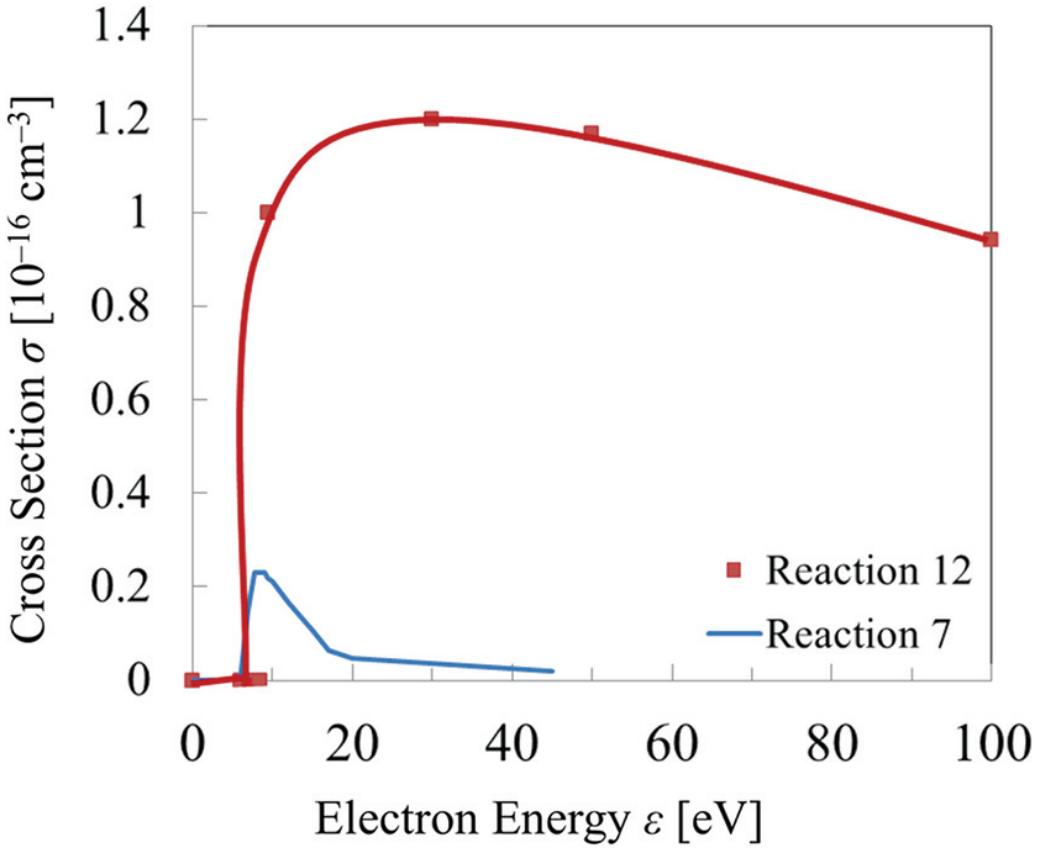

Figure 5: Comparison of electron collision dissociation cross sections of reaction No. 7 and No. 12 in Table 1.

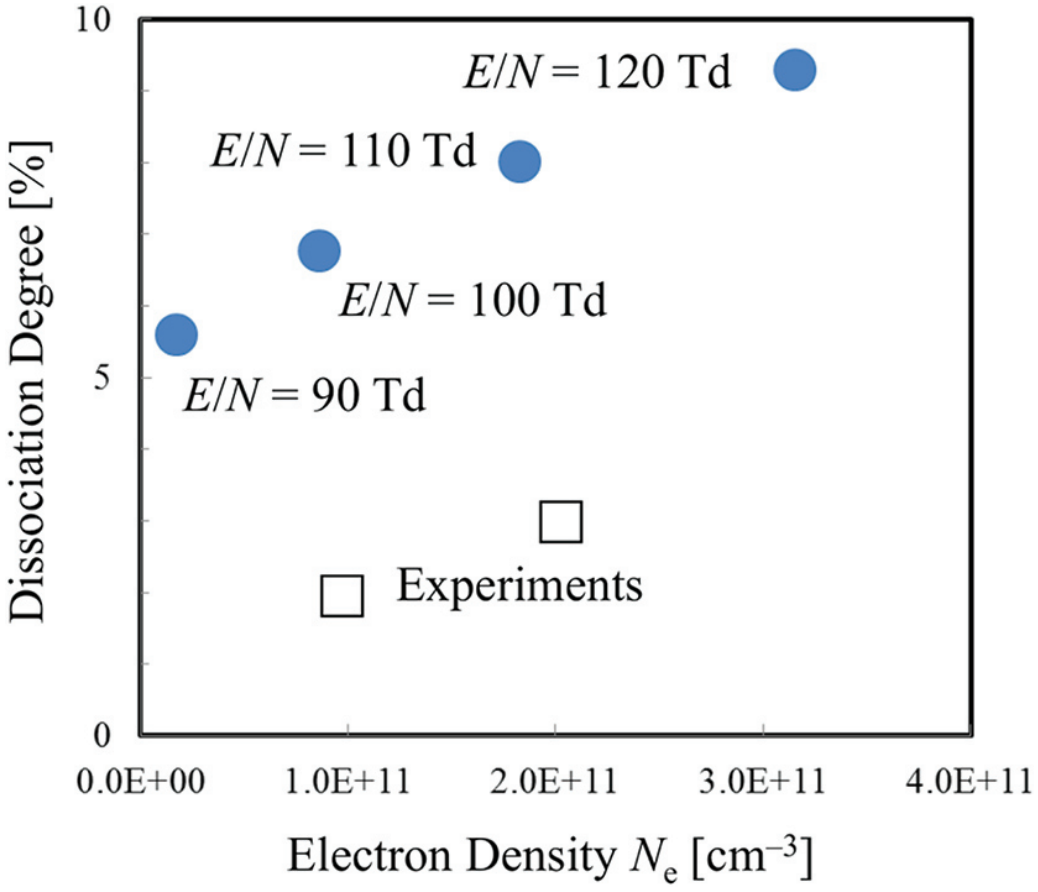

Figure 6: Comparison of the calculated and measured relationships between electron density and dissociation degree of the oxygen plasma.

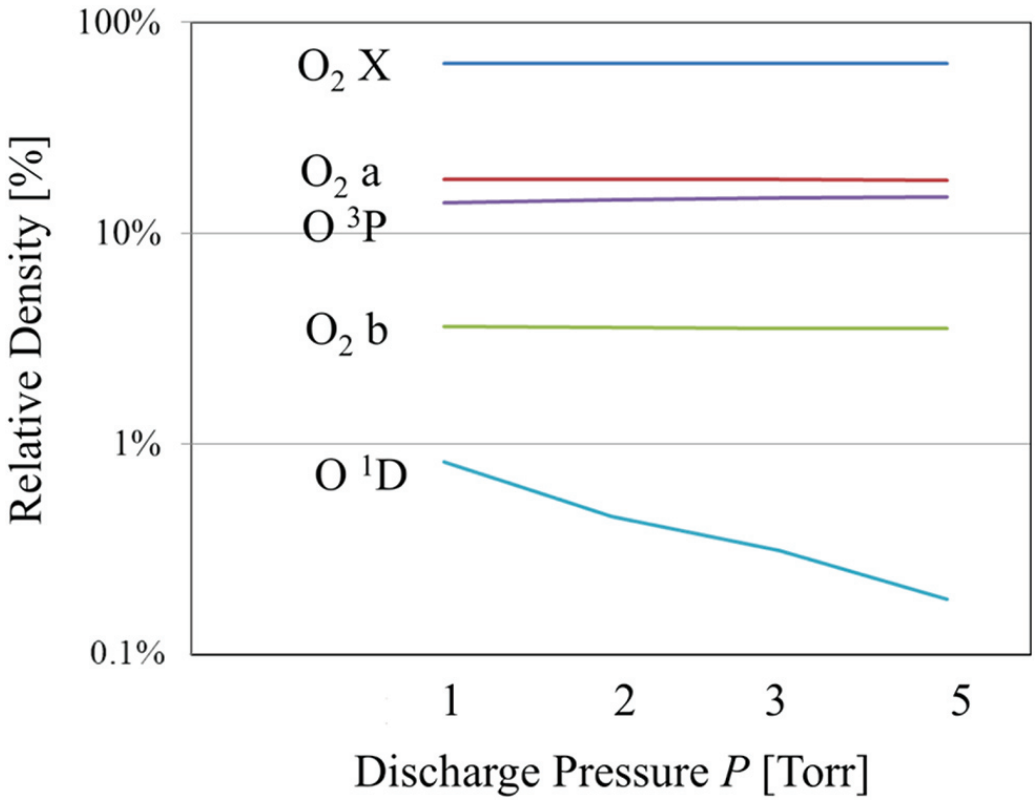

Figure 7: Numerical result of pressure dependence of relative number densities of major species in oxygen plasma. T_g = 0.15 eV, E/N = 110 Td.

5. Summary

On the basis of the essentiality of O(^{1}D) state in the plasma oxidation processes in microelectronics like gate-insulator film preparation, we updated our previous numerical kinetic modeling of excitation kinetics of oxygen plasma with its discharge pressure 1 – 5 Torr. In the present modeling, we calculated the number density of main excited species of oxygen, where we newly added the state O (^{1}D) and considered the population and depopulation of excited species in terms of atomic and molecular processes in the discharge tube. In the present model, we treated O_2 ($X\ ^3\Sigma_g^-$), O_2 ($a\ ^1\Delta_g$), O_2 ($b\ ^1\Sigma_g^+$), O (^{3}P), O_2^+, O^-, O_3, e^- and O (^{1}D), the last of which was newly added in the present study. Based on our numerical kinetic modeling, we calculated their number densities as functions of the reduced electric field, gas discharge pressure, discharge tube radius, and the gas temperature, and discussed the results from the viewpoint of atomic and molecular processes in the plasma. In the numerical model, we simultaneously solved the Boltzmann equation to obtain the self-consistent EEPF, which was also applied to obtain the rate coefficients of various electron impact processes. Its validity of the present numerical model was experimentally examined with the actinometry measurement to obtain the number density of the ground-state oxygen atom O(^{3}P) state. The dissociation degree of O_2 molecule was experimentally found to be 2 – 3 percent, and its qualitative agreement with the numerical model was confirmed, particularly on its dependence on the electron density, although the quantitative exactness was difficult to confirm. Therefore we concluded the qualitative validity of the present modeling of excitation kinetics in the oxygen plasma based on the atomic and molecular processes. We also discussed the theoretical dependence of each excited species on the discharge pressure. As a consequence, if we would like to increase the atomic density ratio of oxygen metastable state O(^{1}D) to the ground state O(^{3}P), which is considered to be crucial for the preparation of high-quality oxide film with oxygen plasma process with its discharge pressure several Torr, we must keep the discharge pressure as low as possible to avoid the collisional relaxation of O(^{1}D) state.

Acknowledgement

The authors thank Mr. Kazuhiro Fujita, Mr. Satoshi Tsuno and Mr. Ryutaro Yamashiro for their eager discussion of this work.

References

1. Lieberman MA, Lichtenberg AJ. Principles of plasma discharges and materials processing, 2nd ed. New York: Wiley, 2005.
2. Fridman A. Plasma chemistry. Cambridge: Cambridge University Press, 2012.
3. Kitajima T, Nakano T, Makabe T. Appl Phys Lett. 2006;88(9) 091501.
4. Sakamoto T, Matsuura H, Akatsuka H. J Adv Oxid Technol. 2007;10(2):247–252.
5. Ichikawa Y, Sakamoto T, Matsuura H, Akatsuka H. Jpn J Appl Phys. 2010;49(10):106101.
6. Tan H, Nezu A, Akatsuka H. Jpn J Appl Phys. 2015;54(9):096103.
7. Kashiwazaki R, Akatsuka H. Jpn J Appl Phys. 2002;41(8):5432–5441.
8. Mizuochi J, Sakamoto T, Matsuura H, Akatsuka H. Jpn J Appl Phys. 2010;49(3):036001.
9. Capitelli M, Ferreira CM, Gordiets BF, Osipov AI. Plasma kinetics in atmospheric gases. Berlin: Springer Verlag, 2000.
10. Akatsuka H. "Progresses in Experimental Study of N_2 Plasma Diagnostics by Optical Emission Spectroscopy", Ch. 13 of "Chemical Kinetics", Ed. by Patel, V.; InTech, Rijeka, Croatia. 2013.
11. Braginsky OV, Vasilieva AN, Klopovsky KS, Kovalev AS, Lopaev DV, Proshina OV, et al. J Phys D. 2005;38(19):3609–3625.
12. Phelps AV. Tabulations of collision cross sections and calculated transport and reaction coefficients for electron collisions with O_2, 1985 JILA Information Center Report, No. 28, Univ. Colorado.
13. Gousset G, Ferreira CM, Pinheiro M, Sa PA, Touzeau M, Vialle M, et al. J Phys D. 1991;24(3):290–300.
14. Yurova IY, Ivanov VE. [in Russian]. "Cross Sections for Scattering of Electrons by Atmospheric Gases", Nauka, Leningrad. 1989.
15. Sakamoto T, Matsuura H, Akatsuka H. J Appl Phys. 2007;101(2):023307.
16. Ricard A, Barbeau C, Besner A, Hubert J, Margot-Chaker J, Moisan M, et al. Can J Phys. 1988;66(8):740–748.